

# Near-field imaging of high-frequency magnetic fields with calorimetric cantilever probes

S. Lee and Y. C. Lee

*Department of Mechanical Engineering, University of Colorado, Boulder, Colorado 80309*

T. M. Wallis,<sup>a)</sup> J. Moreland, and P. Kabos

*National Institute of Standards and Technology, Boulder, Colorado 80305*

(Presented on 2 November 2005; published online 21 April 2006)

Calorimetric probes for near-field imaging of high-frequency (1–20 GHz) magnetic fields were fabricated by depositing patterned metal structures on micromachined, dielectric multilayer cantilevers. In the presence of high-frequency magnetic fields, the metal structures are heated via the generation of eddy currents or via ferromagnetic resonance (FMR). Measurement of the resulting cantilever deflection as a function of probe position produces a map of the microwave power distribution. Comparative measurements from probes with 5 and 10  $\mu\text{m}$  Au rings show that the rings are the active area for eddy current generation. Probes with 10  $\mu\text{m}$  square permalloy patches function in both the eddy current and FMR imaging modes. © 2006 American Institute of Physics. [DOI: 10.1063/1.2167627]

## I. INTRODUCTION

Recently, there has been increasing interest in systems that image high-frequency, electromagnetic fields in the near-field regime.<sup>1</sup> This interest is motivated by applications that include measurements of material properties as well as the characterization of high-frequency circuits. Scanning evanescent microwave microscopes based on sharp probe tips protruding from the center conductor of coaxial microwave<sup>2,3</sup> or microstrip<sup>4</sup> resonators have been used almost exclusively for measuring material properties. Other traditional<sup>5</sup> and apertureless<sup>6</sup> scanning near-field microwave microscopes have also been used for material characterization. However, relatively few probes<sup>1,7</sup> have been developed for direct measurement of magnetic fields emitted by high-frequency/high-speed circuits. In particular, there is a paucity of systems that combine the spatial resolution of scanning probe microscopes with high-frequency compatibility and broad bandwidth.

An additional technique for measuring magnetic fields emitted by high-frequency devices employs micromachined multilayer cantilevers for calorimetric detection of microwave power.<sup>8–10</sup> These magnetic-field sensors consist of a patterned, thin metal film deposited on a dielectric multilayer cantilever. The metal film sensor absorbs microwave power via two mechanisms: (i) via the generation of eddy currents and (ii) if the film is ferromagnetic and an appropriate bias field is applied, through excitation of ferromagnetic resonance (FMR). The resulting heating of the film leads to a measurable deflection of the multilayer cantilever. Two complementary imaging modes arise from the two absorption mechanisms, each with unique advantages: eddy current and FMR imaging.<sup>10</sup> Whereas the FMR imaging mode is a resonant, albeit tunable technique, the eddy current imaging mode is broadband. Additionally, the eddy current imaging

mode allows probes fabricated with nonmagnetic films and no bias field is required. As the lateral resolution of this imaging technique tracks the dimensions of the patterned film, the dimensions of the film must be minimized to achieve useful spatial resolution. This requires optimization of the sensitivity of the cantilever, since a smaller structure will absorb significantly less power.

Here, we report the fabrication of calorimetric magnetic-field probes consisting of individual patterned metal films with dimensions of 5–10  $\mu\text{m}$  deposited on the end of asymmetric, trilayer dielectric cantilevers. We demonstrate that probes with patterned Au rings achieve spatial resolution of approximately 10  $\mu\text{m}$  in the eddy current imaging mode. Additionally, we show that the probes with patterned square permalloy (Py) films are compatible with both eddy current and FMR imaging modes, albeit with less sensitivity.

## II. EXPERIMENTS

A schematic diagram of the cantilever probes is shown in Fig. 1(a). The  $500 \times 25 \mu\text{m}^2$  cantilever beams consist of three layers: a 140 nm silicon nitride layer, a 490 nm silicon oxide layer, and a 210 nm silicon nitride layer. The asymmetric trilayer design provides enough free design parameters to maximize cantilever sensitivity while preventing excessive curling of the cantilevers due to internal stresses within the deposited dielectric layers. The first steps in the cantilever fabrication process were the deposition of the three dielectric layers onto a double-sided polished Si(100) wafer. Next, one of three 150-nm-thick structures—(a) a 5  $\mu\text{m}$  inner diameter Au ring (15  $\mu\text{m}$  outer diameter), (b) a 10  $\mu\text{m}$  inner diameter Au ring (20  $\mu\text{m}$  outer diameter), or (c) a 10  $\mu\text{m}$  square Py patch—was patterned at each cantilever location by the use of a lift-off technique. Thus, three probe types were used, each corresponding to one of the patterned structures: 5  $\mu\text{m}$  Au-ring probes, 10  $\mu\text{m}$  Au-ring probes, and Py square probes. The boundaries of the cantilever were then

<sup>a)</sup>Electronic mail: mwallis@boulder.nist.gov

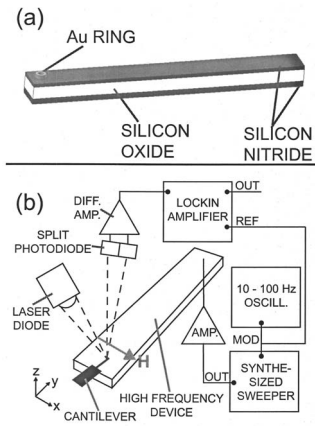


FIG. 1. Schematics of (a) the trilayer cantilever ( $25\ \mu\text{m}$  wide,  $500\ \mu\text{m}$  long) and (b) the experimental apparatus. In (b),  $H$  denotes an applied magnetic bias field for FMR measurements.

photolithographically defined and etched. Finally, the cantilevers were released by dry deep reactive ion etching followed by anisotropic wet etching in KOH. Details of the fabrication process and the optimization of the fabrication parameters will be discussed in a forthcoming paper.<sup>11</sup>

A schematic diagram of the experimental apparatus is shown in Fig. 1(b). The multilayer cantilever sensor was positioned at a fixed height of about  $100\ \mu\text{m}$  above a high-frequency device. Cantilever deflection was detected via a beam-bounce system that consists of light from a diode laser focused onto the end of the cantilever and reflected onto a split photodiode detector. The cantilever and beam-bounce system were incorporated into a homemade scanning head that was mounted on a commercial piezoelectric stage. A synthesized sweeper was used to drive the high-frequency device. The high-frequency signal was amplitude modulated by a 10–100 Hz sine wave that was in turn used as the reference for lock-in detection of the split photodiode detector difference signal. For each Au-ring probe, the cantilever deflection was measured as a function of microwave power as well as position over the edge of a 9.46 GHz microstrip resonator. For the Py square probe, the deflection was measured as a function of microwave power as well as a function of magnetic bias field supplied by an electromagnet. The bandwidth of the eddy current imaging mode was tested by measuring deflection as a function of signal frequency emitted from a coaxial microwave cable with the end conductor exposed.

### III. RESULTS AND DISCUSSION

The response of the Au-ring sensors in the eddy current mode is shown in Fig. 2(a). Note that the power levels shown in Fig. 2(a) represent the output of the synthesized sweeper before amplification and that the power of the signal driving the microstrip resonator was of the order of tens of milliwatts. The response of the  $5\ \mu\text{m}$  Au-ring probe is linear over the entire range of power levels shown, while the response of the  $10\ \mu\text{m}$  Au-ring probes is linear up to 0.07 mW. Divergence from the linear response is due to deflection of the cantilever beyond its elastic regime. The measured linear response ensures that measurement of cantilever deflection, as

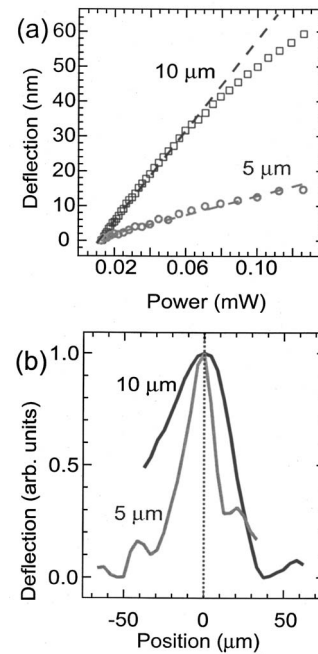


FIG. 2. (a) Cantilever deflection as a function of the power of the driving signal for the  $5\ \mu\text{m}$  Au-ring probe (gray circles) and the  $10\ \mu\text{m}$  Au-ring probe (black squares). Fits to the linear portions of the curves are shown (gray and black dashed lines). (b) Line scans at the edge of a microstrip resonator taken with the  $5\ \mu\text{m}$  Au-ring probe (solid, gray line) and the  $10\ \mu\text{m}$  Au-ring probe (solid, black line). The edge of the resonator is at  $0\ \mu\text{m}$  on the position axis (dotted, black line). The curves have been scaled to facilitate comparison.

a function of probe position, gives an undistorted map of the power of ac magnetic fields emitted by the sample.

In order to demonstrate the imaging capabilities of the Au-ring sensors, line scans were taken across the edge of a microstrip resonator, as shown in Fig. 2(b). The measured profiles of magnetic-field power show a peak in the detected perpendicular component of magnetic field at the resonator's edge. These measurements are consistent with previously measured and calculated field profiles.<sup>9,10</sup> The width of the field profile decreases roughly twofold when the  $5\ \mu\text{m}$  Au-ring probe is used, compared to the  $10\ \mu\text{m}$  Au-ring probe. This demonstrates that the patterned rings are the active area for power absorption via eddy current generation. Thus, the spatial resolution is estimated to be of the order of the dimensions of the Au rings:  $\sim 10\ \mu\text{m}$ . Decreases in the dimensions of the patterned structures will improve the resolution, provided that the corresponding improvements in cantilever sensitivity are made.

The FMR imaging mode is a resonant technique that is tunable via appropriate adjustment of the static biasing magnetic field. Previous experiments have shown that the FMR imaging mode provides a higher signal-to-noise ratio than the eddy current imaging mode, although a biasing field is obviously required.<sup>8–10</sup> It is desirable to produce cantilever probes that can function in both eddy current and the complementary FMR imaging modes. Measurements of deflection of the Py square probe as a function of microwave power emitted by the microstrip resonator in the absence of a bias field are shown in Fig. 3(a). The eddy current response

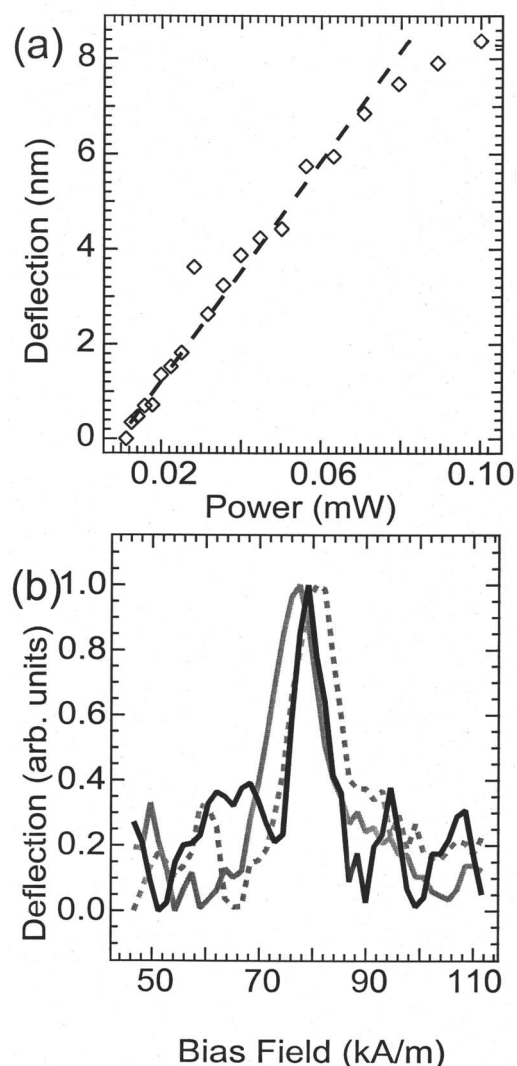


FIG. 3. (a) Cantilever deflection as a function of the power of the driving signal for the Py square probe (black diamonds). A fit to the linear portion of the curve is shown (black dashed line). (b) Cantilever deflection as a function of applied magnetic bias field for the Py square probe when the resonator is driven at 9.36 GHz (gray, solid line), 9.46 GHz (black, solid line), and 9.56 GHz (gray, dashed line). The curves have been scaled to compensate for the frequency dependence of the resonator reflection coefficient.

of the Py square probe is comparable with that of the  $5\ \mu\text{m}$  Au-ring probe. Measurements of the cantilever deflection, as a function of bias field, in the presence of high-frequency radiation show an additional FMR contribution [Fig. 3(b)] at  $79 \pm 2\ \text{kA/m}$  ( $995 \pm 20\ \text{Oe}$ ) when placed above the microstrip resonator operating at the resonant frequency of 9.46 GHz. Expected shifts in the peak position are observed when the driving signal frequency is shifted to 9.36 and 9.56 GHz. The signal-to-noise ratio for the data shown in Fig. 3(b) is significantly poorer than that reported in Refs. 8 and 9. This is attributed to the decreased volume of the ferromagnetic film as well as to differences between the commercial scanning head used previously and the homemade scanning head used here.

Eddy current imaging of microwave power emitted by high-frequency/high-speed circuits is an attractive, noncontact imaging technique due largely to its broad bandwidth. Deflection of Au-ring probes due to eddy current generation in the presence of a coaxial microwave cable with the end conductor exposed was found to be sufficient for imaging in the 5–20 GHz range. Though induced eddy currents vary linearly with frequency according to Faraday's Law, the frequency dependence was determined largely by the reflection coefficient of the high-frequency device and the properties of the driving microwave network. The primary drawback of this technique is that the thermal time constants required for calorimetric detection lead to long scan times and prevent amplitude modulation at the cantilever's mechanical resonance frequency. Images produced with calorimetric techniques reveal spatially resolved contrast in microwave power, but are difficult to interpret quantitatively. Direct field measurement techniques that use microfabricated antennas will be required to quantitatively image devices that emit radiation at lower power levels.

#### IV. CONCLUSIONS

Calorimetric detection of microwave power with multilayer cantilever sensors provides two complementary imaging modes. The eddy current imaging mode provides a noncontact, broadband imaging technique while the FMR mode provides a resonant, albeit tunable technique. Decreases in the size of patterned Au rings incorporated into calorimetric probes improve resolution. Py square probes function in both the eddy current and FMR imaging modes. The FMR response of the Py square probes opens the possibility of integrating the high-frequency source into the scanning head in order to perform on-chip investigations of the dynamic response of individual patterned magnetic structures.

#### ACKNOWLEDGMENT

This work was partially supported by the National Institute of Standards and Technology.

<sup>1</sup>B. T. Rosner and D. W. van der Weide, *Rev. Sci. Instrum.* **73**, 2505 (2002).

<sup>2</sup>A. Imtiaz, M. Pollak, S. M. Anlage, J. D. Barry, and J. Melngailis, *J. Appl. Phys.* **97**, 044302 (2005).

<sup>3</sup>C. Gao and X.-D. Xiang, *Rev. Sci. Instrum.* **69**, 3846 (1998).

<sup>4</sup>R. Wang, F. Li, and M. Tabib-Azar, *Rev. Sci. Instrum.* **76**, 054701 (2005).

<sup>5</sup>M. Golosovsky, A. F. Lann, D. Davidov, and A. Frankel, *Rev. Sci. Instrum.* **71**, 3927 (2000).

<sup>6</sup>B. Knoll and F. Keilmann, *Nature (London)* **399**, 134 (1999).

<sup>7</sup>B. T. Rosner, T. Bork, V. Agrawal, and D. W. van der Weide, *Sens. Actuators, A* **102**, 185 (2002).

<sup>8</sup>J. Moreland, M. Lohndorf, P. Kabos, and R. D. McMichael, *Rev. Sci. Instrum.* **71**, 3099 (2000).

<sup>9</sup>A. Jander, J. Moreland, and P. Kabos, *J. Appl. Phys.* **89**, 7086 (2001).

<sup>10</sup>T. M. Wallis, J. Moreland, B. Riddle, and P. Kabos, *J. Magn. Magn. Mater.* **386**, 320 (2005).

<sup>11</sup>S. Lee, T. M. Wallis, J. Moreland, P. Kabos, and Y. C. Lee (unpublished).